

A Self-Assembling Peptide Polyanoreactor**

Maxim G. Ryadnov*

Biomolecular self-assembly has been increasingly applied to the fabrication of novel supramolecular structures.^[1] The approach allows the construction of a supramolecular composite or its components from the bottom up, a route that offers the potential to define and control the properties of the resulting materials at the nanometer scale. Nanoreactors particularly benefit from this, as their key function—deposition of a reaction or a material—is intimately associated with confining a reaction environment.^[2] It becomes even more critical in designing a nanoreactor with multiple reaction sites, which has yet to be reported. Herein, a new design is described that allows the amplification of a discrete material within an individual nanoreactor; that is, it acts as a “polynanoreactor”. The system results from a noncovalent dendrimer-like assembly of short leucine zipper sequences.^[3,4] The designed polynanoreactors host numerous nanosized cavities that are demonstrated to function as encapsulating sites in casting copious uniformly sized silver nanoparticles.

A prerequisite for all types of nanoreactors is encapsulation,^[2] that is, an ability to form and sustain cavities capable of hosting or encapsulating guest materials. Designing a nanoreactor with multiple cavities introduces a higher level of complexity, which eventually determines the choice of a molecular candidate. One molecular class that meets these requirements is self-assembled dendrimers, which have been extensively exploited over the last two decades.^[5,6] Pioneering studies by Zimmerman et al.,^[7] Percec et al.,^[8] Tomalia and co-workers,^[9] Hecht and Fréchet,^[10] and Meijer and co-workers^[11] on supramolecular dendrimer systems offer a strong basis to apply the properties of the dendritic state to engineering nanoreactors. Most remarkably, the properties of such systems are reminiscent of those displayed by natural nanoreactors such as ribosomes, enzyme complexes, and protein cages.^[2] Therefore, the main drive of the present study in designing polyananoreactors is to express dendrimer architectures by a “natural” self-assembly motif.

The polyanoreactors were designed in two steps. The first step consisted of building a noncovalent dendrimer framework, which is referred to herein as a supradendrimer (SD). This SD is obtained from the self-assembly of a single peptide sequence, SD-1 (Figure 1A), which is based on a dimeric coiled coil also known as the leucine zipper. It is one of the most abundant assembling motifs in natural biosystems and presents a bundle of two α helices.^[3] Amino acid preferences that distinguish between the character and oligomerization state of the bundle can be rationally specified

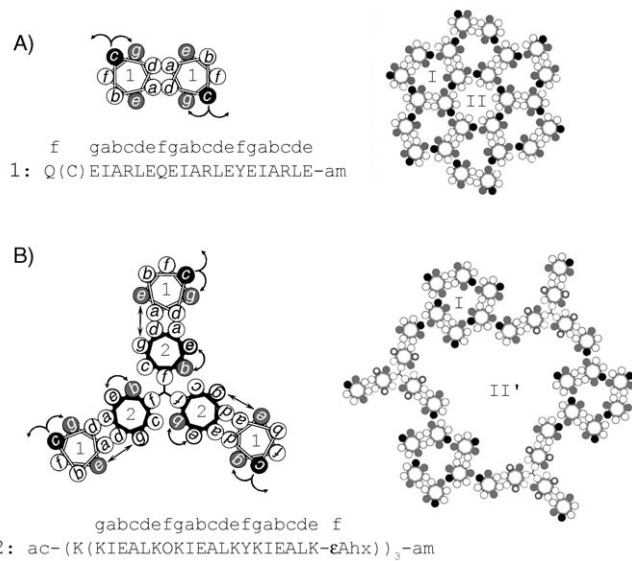


Figure 1. Schematic representation of the supradendrimer design. SD-1 (1) and SD-2 (2) peptide sequences are shown with the one-letter code and are simplified into helical wheels with 3.5 residues per turn.^[3] The sequences show heptad repeats characteristic of canonical coiled coils, commonly labeled *a*–*g*. Residues at sites *a* and *d* shape helix–helix interfaces. These are hydrophobic and made up of isoleucine and leucine, respectively, to ensure the formation of dimers.^[4] A) SD-1-type of electrostatic interactions, *g*–*c*–*e*': *e*' and *g* positions are occupied by glutamates that form salt bridges with arginine residues at *c*; *g*–*c* interactions are intrahelical, whereas *c*–*e*' are interhelical and are between two SD-1 copies of different dimers. Dimers trimerize (I) to give a noncovalent dendrimeric architecture, with a branching cell formed by six dimers (II). A single cysteine residue in the *f* position that replaces a glutamine is shown in brackets. B) Mixed SD-1/SD-2 (SD-1,2)-type of electrostatic interactions, *g*–*c*–*e*'(1)/*b*–*e*, *g*–*e*'(2): intra-helical *b*–*e* interactions in 2 inhibit interhelical *e*'–*g*' interactions; *g*–*e*' interactions contribute to the 1–2 interface. Because the width of a superhelix is approximately 2 nm, the diameter of an extended branching cell (II') is estimated to not exceed 4–6 nm. To form the supradendrimer II', each copy of SD-2 should be arranged with at least nine copies of SD-1 to round the equimolar SD-1,2 ratio to 10:1. SD-2 wheels are highlighted in black around an ac-KKK-am hub containing an ϵ -aminohexanoic acid (ϵ Ahx) as spacer. The circles of helical wheels are black for arginines, gray for glutamates, and outlined in gray for lysines. Arrows represent salt bridges.

[*] Dr. M. G. Ryadnov
School of Chemistry
University of Bristol
Bristol BS8 1TS (UK)
Fax: (+44) 117-925-1295
E-mail: max.ryadnov@bristol.ac.uk

[**] I thank Dek N. Woolfson (D.N.W.) for encouragement and support; the D.N.W. group for fruitful discussions on the content and presentation of this work; and Gini Tilly, Deborah Carter, Jon Jones, and Sean Davis for technical assistance with TEM. This work was funded partly by a pump-priming grant from the Cancer Research Fund (University of Bristol) and partly by a start-up grant (to D.N.W.) for establishing Protein Design Laboratories in Bristol.

 Supporting information for this article is available on the WWW under <http://www.angewandte.org> or from the author.

that facilitate their design.^[4] Coiled coils are amphipathic and exhibit a heptad repeat in chemistry of their side chains: HPPHPPP (H = hydrophobic, P = polar).^[3] The hydrophobic face of SD-1 was set to support formation of a homodimer^[3,4] (Figure 1 A). Polar sites were transformed into two polar faces to create a network of electrostatic interactions that favor associations *between* dimers rather than within a single dimer (Figure 1 A)—the key feature of the design.

To this end, arginine residues were put into the *c* positions of the heptad repeat to form intra- and interhelical bridges with glutamates. The guanidinium group of each arginine residue can form two salt bridges with two carboxylate groups. In essence, the principle applies Crick's critical assumptions on the interface packing of hydrophobic faces^[12] in coiled coils to the packing of polar faces. Findings from other researchers, notably from Hodges and co-workers^[13] and Burkhard et al.,^[14] who have consistently shown the impact of multiple intra- and interhelical interactions on the stability of coiled coils, also underpin the design. Others proposed similar approaches to obtain more-complex supramolecular structures by introducing offsets of interhelical salt bridges^[15] or bifaceted hydrophobic seams^[16,17] inspired by the structure of the membrane protein TolC.^[18] In these designs, as well as in most others, polar residues in the interacting *g* and *e* sites contribute to the helix–helix interface. In contrast, in the supradendrimers presented here, *g* and *e* sites are occupied by the residues of the same polarity (glutamates) which excludes their direct participation in the formation of dimers. Within a hypothetical dimer, repulsion between glutamates is partly neutralized by arginine residues at *c* (*i*) sites that take on glutamates at *g* (*i* + 4) sites.^[13,14] Free glutamates at *e* sites can produce further salt bridges provided there is a spatial arrangement that allows them to interact with oppositely charged arginines.^[14] Thus, one arginine residue links a *g* glutamate of the same helix with an *e* glutamate of another helix (*e'*) of another dimer. The formation of individual dimers is supported by their organization into a larger cluster, which has a repetitive unit. The unit comprises a branching cell of six dimers arranged in a starburst fashion and each of which is shared by adjacent cells. Given the minimum requirement of three contiguous heptads to form stable assemblies,^[19] an SD-1 sequence (QEIARLE-QEIARLEYEIARLE-am) summarizes the design principles (Figure 1 A).

When folded, SD-1 dimers are rigid rods,^[3] that is, assembled anisotropically. However, as their self-assembly starts and is sustained by the formation of hollow dendrimer cells, the rods extend into tightly packed noncovalent networks. Because the networks are long-range assemblies of identical subunits, some level of symmetry should be expected; that is, SD-1 dimers pack symmetrically and each dimer is provided with an identical structural environment,^[20] which in turn requires a high level of cooperativity of dimers and network ordering.

Consistent with the design, SD-1 assembled cooperatively as probed by circular dichroism (CD) spectroscopy (see the Supporting Information). Transmission electron microscopy (TEM) revealed very dense mesoscopic assemblies of a hexagonal paracrystalline phase, which concurs with the

spectroscopic data to suggest a hierarchically ordered architecture of SD-1 supradendrimers (Figure 2 A and C).^[21] In contrast, control sequences (QEIAALEQEIAALEYEIALE-am and QEIAKLEQEIAKLEYEIAKLE-am), in which arginine residues were replaced by alanine and lysine residues, respectively, to eliminate electrostatic networks consolidated by arginines, neither folded nor underwent self-assembly (see Figure S2a in the Supporting Information).

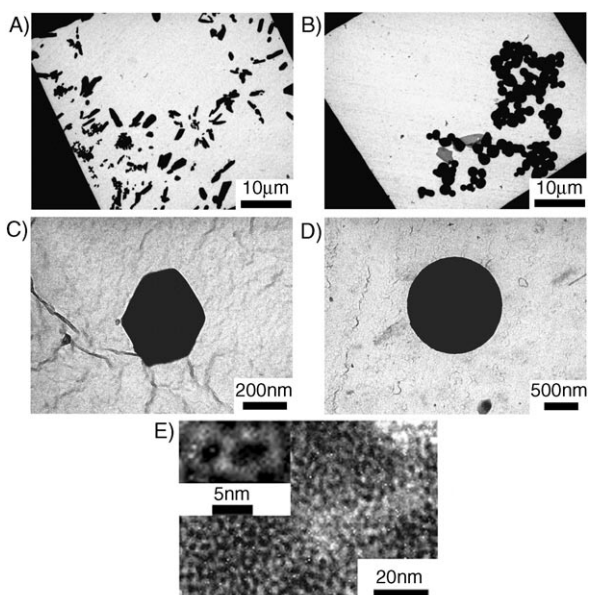


Figure 2. TEM images of SD-1 (A and C) and SD-1,2 (B and D) supradendrimers. E) The surface pattern of SD-1,2; the inset shows two overlapping rings with a mean diameter of (4.6 ± 0.7) nm.

Self-assembled dendrimers are dynamic supramolecules with enhanced properties characteristic of the dendritic state.^[5] Such properties are largely entropy-driven and can be drastically affected by the chemical potential.^[5–11] This is particularly important for encapsulation. Encapsulation in dendrimers is acquired upon reaching a certain size usually defined as a higher generation in dendrimer architectures.^[8–11] SD-1 supradendrimers are high-generation dendrimers that are formed by condensed networks of cooperatively folded rodlike superhelices. Within a network, the superhelices are arranged to form nanoscopic cavities presented by the cores of noncovalent branching units (Figure 1 A). The ordering of dense networks within a supradendrimer implies a mechanical sustainability of the formed cavities. However, tightly meshed SD-1 dimers, which are 2-nm wide and 3-nm long, may compromise the size and stability of smaller branching cells as hosts.

With this in mind to engineer a distinguishable cavity, branching cells were extended by incorporating another subunit to SD-1 supradendrimers (Figure 1 B), thus outlining the second step of the design—to introduce encapsulation. SD-2 presents a leucine zipper sequence that is complementary to SD-1, and SD-2 assembles with SD-1 into an SD-1,2 dimer. The dimer is designed to be compatible with the

network of the electrostatic interactions of SD-1. An additional constraint was set to direct and foster the formation of cavities; SD-2 was covalently triplicated into a starburst molecule (Figure 1B).

The SD-2 sequence follows the same principles applied in SD-1 (Figure 1). The autonomous folding of SD-2 is strongly discouraged by lysine residues at the *e* and *g* positions, with one lysine at *e* (*i*) neutralized by a glutamate at *b* (*i*+3). Unlike arginine, lysine can support only one salt bridge, thus preventing SD-2 from building interhelical salt bridges as SD-1 does. SD-2 has two polar faces that form a network of electrostatic interactions only in a mixture with SD-1 (Figure 1B). Accordingly, CD measurements revealed no appreciable α helix for SD-2 (see Figure S1 in the Supporting Information) and no assemblies were observed by TEM. Notwithstanding certain similarities, the assembly mode of SD-1 with SD-2 is different from that of SD-1 with itself. A more complex network of salt bridges is maintained: *g*-*e'* interactions between SD-2 and SD-1 helices contribute to the coiled-coil interface, whereas *e*-*g'* interactions are inhibited by intrahelical *b*-*e* interactions of SD-2 and *c*-*g* interactions of SD-1, which support *c*-*e'* interactions between SD-1 helices of SD-1,2 and SD-1 dimers. The *g*-*e'* interactions are thermodynamically most favorable,^[3,4] as is the co-assembly of SD-1 and SD-2, which therefore brings a synergistic effect to the assembly, without competition between the SD-1,2 and SD-1 superhelices.

Indeed, SD-1,2 showed a cooperatively and reversibly folded helical structure comparable with that of SD-1, (see Figure S1 in the Supporting Information). Perfectly ball-shaped paracrystals that reformed following annealing were detected by TEM (Figure 2B and D). The assemblies were almost uniformly sized with an average diameter of (1.4 ± 0.4) μ m (see Figure S4 in the Supporting Information). Consistent with the extended branching cells, SD-1,2 supradendrimers were larger than SD-1 supradendrimers.

Paracrystals are characterized by a crystalline internal order,^[22] which is often accompanied by specific surface features.^[21] In this regard, it was possible to detect a pattern on the surfaces of SD-1,2 supradendrimers that, however, was only apparent for partly disintegrated or opened up assemblies (see Figure S5 in the Supporting Information). Detailed TEM examinations of SD-1,2 surfaces revealed overlapping rings with an average size of (4.6 ± 0.7) nm (Figure 2E as well as Figure S4 in the Supporting Information). This observation is in a good agreement with the estimated diameter of the branching cells of SD-1,2 (Figure 1B).

To demonstrate whether the extended cells can be used as encapsulants, a metal redox reaction was chosen. Since the seminal studies by Mann and co-workers in the early 1990s,^[23] the redox chemistry of metal ions has been explored as the most straightforward approach for the synthesis of nanomaterials in proteinaceous nanoreactors.^[24] Examples include *in situ* redox switching in ferritins,^[23] syntheses of nanoparticles in protein^[25] and viral^[26] cages, and casting nanowires in nanotubes.^[27] In this context, the cavities of SD-1,2 mimic the constrained environments of natural protein vessels to template the conversion of ionic into colloidal metals, for example, in the synthesis of nanoparticles. Complementarily,

thiols were shown to have a size-stabilizing effect on the resulting metallic nanocomposites in a series of studies.^[28,29] The effect also appeared to correlate with the length of thiolated molecules.^[29] With this effect taken into account, the SD-1,2 system was supplemented with thiol components: the N-terminal glutamine of SD-1 was replaced by a cysteine residue (Figure 1A and the Supporting Information). This position is also an *f* position in the coiled coil, which guarantees the required orientation of cysteine residues inwards with respect to the branching core, that is, the reactor (Figure 3A and the Supporting Information).

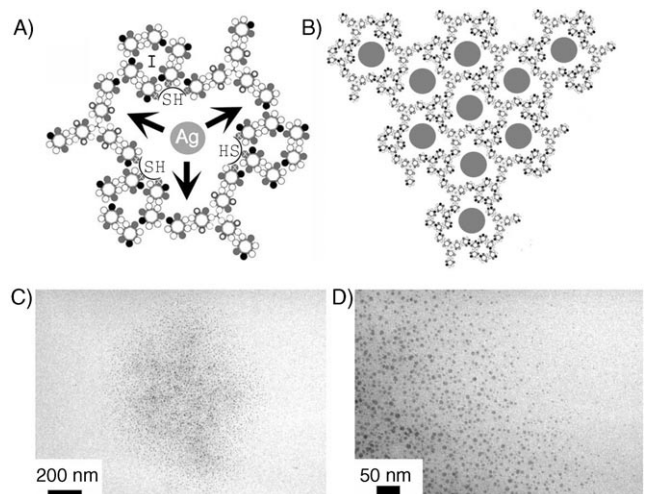


Figure 3. Synthesis of silver nanoparticles within SD-1,2. A) A growing silver nanoparticle (Ag) hosted by an SD-1,2 cavity is depicted as a gray circle. B) A network of cavities filled with silver nanoparticles (gray circles). Arrows indicate the confined space of the cavity within which the particle is to grow. Cysteine residues forming encapsulating thiol (SH) clusters are shown as circles marked with crosses. C) An electron micrograph of a spherical 1.2- μ m wide spread of silver nanoparticles. D) High magnification of an edge portion of the image shown in part (C). See also Figure S7 in the Supporting Information.

A conventional citrate reduction method for colloidal gold^[28] in combination with a recently reported method for casting silver nanowires^[27] was adapted. Briefly, a nearly boiling solution of silver nitrate was added to an SD-1,2 preparation followed by the immediate addition of sodium citrate as reducing reagent. Following incubation of the preparation with chymotrypsin, TEM analysis revealed sub-micron-to-micron spreads of individual nanoparticles (Figure 3B). The narrow distribution of diameters of the individual nanoparticles was consistent with that of the cavities, as was the average diameter of nanoparticles, (5.2 ± 0.5) nm, compared to that of the nanorings constituting the cavities (see Figure S4 in the Supporting Information). The results indicate that SD-1,2 supradendrimers amplify a material, such as silver nanoparticles in the present case, with the designed cavities serving as multiple reaction sites. This result supports the function of SD-1,2 as a polyanoreactor by design.

In summary, a new type of self-assembling peptide-based nanoreactor has been described. By hosting multiple reaction

sites, each nanoreactor produces copious amounts of materials with nanometer dimensions, thus serving as a polyananoreactor. With the demonstrated potential of controlling the size of such sites, the design constitutes a precedent of a system with a tunable and sustainable interior that provides a constrained reaction environment on the nanoscale.

Experimental Section

Peptide preparation, assembly, and biophysics: Peptides were assembled on a solid phase using Fmoc (9-fluorenylmethoxycarbonyl) protocols, purified by reverse-phase high-pressure liquid chromatography, and analyzed by mass spectrometry (see the Supporting Information). Aqueous preparations of SD (200 μ L, 10–100 μ M) were made in filtered (0.22 μ m) 10 mM MOPS (morpholinepropanesulfonic acid) containing 0.02% sodium azide, pH 7.0–7.4 (unless otherwise stated), and incubated for 30 min to 16 h at 20°C. Circular dichroism spectroscopy was performed on a JASCO J-810 spectropolarimeter fitted with a Peltier temperature controller. All measurements were taken in ellipticities (mdeg) and converted into molar ellipticities ($\theta/\text{deg cm}^2 \text{dmol res}^{-1}$) by normalizing for the concentration of peptide bonds. Thermal denaturation curves were recorded at 1°C intervals using a bandwidth of 1 nm, with the signal averaged for 16 s, and a ramp rate of 1°C min⁻¹.

Electron microscopy: Following incubation, 8- μ L drops of peptide solutions were applied to carbon-coated copper specimen grids (Agar Scientific) and dried. The grids were examined without staining in a JEOL JEM 1200 EX MKI microscope at the accelerating voltage of 100 kV. Images were digitally acquired with a fitted camera (MegaViewII).

Synthesis of silver nanoparticles: Silver nanoparticles were prepared by a citrate reduction of silver nitrate. A nearly boiling aqueous solution of silver nitrate (10 mM, 5 μ L) was added to a matured preparation of SD-1.2 (0.1 mM, 95 μ L) at room temperature. Immediate titration of this mixture with trisodium citrate (final concentration 0.05–0.1%) was followed by a 1–3 h incubation with chymotrypsin at 37°C. The resulting preparations were analyzed by TEM without staining.

Received: September 29, 2006

Revised: October 28, 2006

Published online: December 13, 2006

Keywords: dendrimers · nanoreactors · noncovalent interactions · peptides · self-assembly

- [1] *Nanobiotechnology: Concepts, Applications and Perspectives* (Eds.: C. M. Niemeyer, C. A. Mirkin), Wiley-VCH, Weinheim, 2004.

- [2] D. M. Vriezema, M. Comellas Aragones, J. A. A. W. Elemans, J. J. L. M. Cornelissen, A. E. Rowan, R. J. M. Nolte, *Chem. Rev.* **2005**, *105*, 1445–1490.
- [3] A. N. Lupas, M. Gruber, *Adv. Protein Chem.*, Vol. 70, Academic Press, New York, **2005**, pp. 37–78.
- [4] D. N. Woolfson, *Adv. Protein Chem.*, Vol. 70, Academic Press, New York, **2005**, pp. 79–112.
- [5] J. M. J. Fréchet, *Proc. Natl. Acad. Sci. USA* **2002**, *99*, 4782–4787.
- [6] S. Svenson, D. A. Tomalia, *Adv. Drug Delivery Rev.* **2005**, *57*, 2106–2129.
- [7] S. C. Zimmerman, F. Zeng, D. E. C. Reichert, S. V. Kolotuchin, *Science* **1996**, *271*, 1095–1098.
- [8] V. Percec, W.-D. Cho, P. E. Mosier, G. Ungar, D. J. P. Yeardley, *J. Am. Chem. Soc.* **1998**, *120*, 11061–11070.
- [9] S. Uppuluri, D. R. Swanson, L. T. Piehler, J. Li, G. L. Hagnauer, D. A. Tomalia, *Adv. Mater.* **2000**, *12*, 796–800.
- [10] S. Hecht, J. M. J. Fréchet, *Angew. Chem.* **2001**, *113*, 76–94; *Angew. Chem. Int. Ed.* **2001**, *40*, 74–91.
- [11] R. M. Versteegen, D. J. M. van Beek, R. P. Sijbesma, D. Vlassopoulos, G. Fytas, E. W. Meijer, *J. Am. Chem. Soc.* **2005**, *127*, 13862–13868.
- [12] F. H. C. Crick, *Acta Crystallogr.* **1953**, *6*, 689–697.
- [13] M. E. Houston, A. P. Campbell, B. Lix, C. M. Kay, B. D. Sykes, R. S. Hodges, *Biochemistry* **1996**, *35*, 10041–10050.
- [14] P. Burkhard, S. Ivaninskii, A. Lustig, *J. Mol. Biol.* **2002**, *318*, 901–910.
- [15] A. M. Smith, E. F. Banwell, W. R. Edwards, M. J. Pandya, D. N. Woolfson, *Adv. Funct. Mater.* **2006**, *16*, 1022–1030.
- [16] J. Walshaw, D. N. Woolfson, *Protein Sci.* **2001**, *10*, 668–673.
- [17] D. E. Wagner, C. L. Phillips, W. M. Ali, G. E. Nybakken, E. D. Crawford, A. D. Schwab, W. F. Smith, R. Fairman, *Proc. Natl. Acad. Sci. USA* **2005**, *102*, 12656–12661.
- [18] V. Koronakis, A. Sharff, E. Koronakis, B. Luisi, C. Hughes, *Nature* **2000**, *405*, 914–919.
- [19] J. Su, R. S. Hodges, C. M. Kay, *Biochemistry* **1994**, *33*, 15501–15510.
- [20] F. H. C. Crick, J. D. Watson, *Nature* **1956**, *177*, 473–475.
- [21] H. Herrmann, U. Aebi, *Annu. Rev. Biochem.* **2004**, *73*, 749–789.
- [22] A. M. Hindeleh, R. Hosemann, *J. Phys. C* **1988**, *21*, 4155–4170.
- [23] F. C. Meldrum, V. J. Wade, D. L. Nimmo, B. R. Heywood, S. Mann, *Nature* **1991**, *349*, 684–687.
- [24] S. Mann, *Biomineralization: Principles and Concepts in Bioinorganic Materials Chemistry*, Oxford University Press, Oxford, 2002.
- [25] M. Allen, D. Willits, J. Mosolf, M. Young, T. Douglas, *Adv. Mater.* **2002**, *14*, 1562–1565.
- [26] T. Douglas, M. Young, *Nature* **1998**, *393*, 152–155.
- [27] M. Reches, E. Gazit, *Science* **2003**, *300*, 625–627.
- [28] J. Turkevich, P. C. Stevenson, J. Hillier, *Discuss. Faraday Soc.* **1951**, *11*, 55–75.
- [29] M.-C. Daniel, D. Astruc, *Chem. Rev.* **2004**, *104*, 293–346.